

Optical Analysis of the Fine Crystalline Structure of Artificial Opal Films

G. Lozano,[†] L. A. Dorado,[‡] D. Schinca,^{§,||} R. A. Depine,[‡] and H. Míguez^{*,†}[†]Instituto de Ciencia de Materiales de Sevilla, Consejo Superior de Investigaciones Científicas, Sevilla, Spain,[‡]Grupo de Electromagnetismo Aplicado, Departamento de Física, Facultad de Ciencias Exactas y Naturales, Universidad de Buenos Aires, Buenos Aires, Argentina, [§]Centro de Investigaciones Ópticas (CIOp),(CIC-CONICET), La Plata, Argentina, and ^{||}Departamento de Ciencias Básicas, Facultad de Ingeniería, Universidad Nacional de La Plata, Argentina

Received August 18, 2009. Revised Manuscript Received September 29, 2009

Herein, we present a detailed analysis of the structure of artificial opal films. We demonstrate that, rather than the generally assumed face centered cubic lattice of spheres, opal films are better approximated by rhombohedral assemblies of distorted colloids. Detailed analysis of the optical response in a very wide spectral range ($0.4 \leq a/\lambda \leq 2$, where a is the conventional lattice constant), as well as at perpendicular and off-normal directions, unambiguously shows that the interparticle distance coincides very approximately with the expected diameter only along directions contained in the same close-packed plane but differs significantly in directions oblique to the [111] one. A full description of the real and reciprocal lattices of actual opal films is provided, as well as of the photonic band structure of the proposed arrangement. The implications of this distortion in the optical response of the lattice are discussed.

Introduction

Opal-like structures, consisting of lattices of dielectric spheres, are the most commonly studied example of three-dimensional photonic crystals.^{1–3} Since they were proposed as new materials to mold the flow of light, they have become an important area of research because of their technological potential and fundamental interest.⁴ Among all fabrication techniques developed up to date to prepare opaline photonic crystals, those based on evaporation induced self-assembly (EISA) are some of the most frequently employed and thoroughly analyzed.⁵ The introduction of this method⁶ has largely improved the quality of the crystals and made it possible to study for the first time fine optical phenomena.^{7,8} It is also accepted that, using this method, the final result is a compact arrangement of spheres mainly ordered in a face center cubic (FCC) structure.^{9–12} In such packing, the distance between first neighbors does not depend on crystallographic directions. However, some experimental evidence recently reported suggests

the existence of distortion in artificial opal lattices.^{13–16} One of the most conclusive pieces of evidence in this regard is the one obtained by Ishii et al.¹⁵ By analyzing the angular dependence of both the specular reflectance peak associated to the lowest energy pseudogap and the intensity of the backscattered radiation, they could extract information on the average interparticle distance along different crystalline directions and prove the existence of distortion in different types of artificial opal lattices.

The importance of the existence of a certain distortion becomes particularly relevant when the optical response at wavelengths on the same order as the spatial period of the dielectric constant is analyzed. The understanding of the complex optical properties observed in this range has been lively debated during the last years.^{17–22} We have recently provided a detailed analysis and rationalization of a number of reported observations whose cause remained unclear, that is, the physical origin of all the spectral features observed in the specular reflectance and ballistic transmittance spectra, as well as of the intensity variations of the nonspecularly diffracted beams.^{23,24} During the course of these analyses, the difficulty to attain a simultaneous fitting of the optical response in a wide spectral energy range (i.e., $0.4 \leq a/\lambda \leq 2$) using the structural parameters assumed for an FCC lattice became evident,²⁰ which led us to carry out a careful exploration of the reasons behind this. Similar difficulties to achieve good simultaneous fitting of all the features observed in the reflectance and transmittance in that same spectral range have also been found by other groups.²⁵

*To whom correspondence and request of materials should be addressed.
E-mail: hernan@icmse.csic.es.

- (1) Yablonovitch, E. *Phys. Rev. Lett.* **1987**, *58*, 2059.
- (2) John, S. *Phys. Rev. Lett.* **1987**, *58*, 2486.
- (3) López, C. *Adv. Mater.* **2003**, *15*, 1679.
- (4) Blanco, A.; Chomski, E.; Grubbs, S.; Ibisate, M.; John, S.; Leonard, S. W.; López, C.; Meseguer, F.; Míguez, H.; Mondia, J. P.; Ozin, G. A.; Toader, O.; van Driel, H. M. *Nature* **2000**, *405*, 437.
- (5) Lozano, G.; Dorado, L. A.; Depine, R. A.; Míguez, H. *J. Mater. Chem.* **2009**, *19*, 185.
- (6) Jiang, P.; Bertone, J. F.; Hwang, K. S.; Colvin, V. L. *Chem. Mater.* **1999**, *11*, 2132.
- (7) Wong, S.; Kitaev, V.; Ozin, G. A. *J. Am. Chem. Soc.* **2003**, *125*, 15589.
- (8) Wostyn, K.; Zhao, Y.; Yee, B.; Clays, K.; Persoons, A.; de Schaeften, G.; Hellemans, L. *J. Chem. Phys.* **2003**, *118*, 10752.
- (9) Lozano, G.; Míguez, H. *Langmuir* **2007**, *23*, 9933.
- (10) Míguez, H.; Meseguer, F.; López, C.; Mifsud, A.; Moya, J. S.; Vázquez, L. *Langmuir* **1997**, *13*, 6009.
- (11) Norris, D. J.; Arlinghaus, E. G.; Meng, L. L.; Heiny, R.; Scriven, L. E. *Adv. Mater.* **2004**, *16*, 1393.
- (12) Gasperino, D.; Meng, L.; Norris, D. J.; Derby, J. J. *J. Cryst. Growth* **2008**, *310*, 131.
- (13) Gottardo, S.; Burrelli, M.; Geobaldo, F.; Pallavidino, L.; Giorgis, F.; Wiersma, D. S. *Phys. Rev. E* **2006**, *74*, 040702(R).
- (14) García-Santamaría, F.; Braun, P. V. *Appl. Phys. Lett.* **2007**, *90*, 241905.
- (15) Ishii, M.; Harada, M.; Tsukigase, A.; Nakamura, H. *J. Opt. A: Pure Appl. Opt.* **2007**, *9*, S372.

- (16) Popa, I.; Marlow, F. *Chem. Phys. Chem* **2008**, *9*, 1541.
- (17) Míguez, H.; Kitaev, V.; Ozin, G. A. *Appl. Phys. Lett.* **2004**, *84*, 1239.
- (18) Galisteo-López, J. F.; López, C. *Phys. Rev. B* **2004**, *70*, 035108.
- (19) Balestreri, A.; Andreani, L. C.; Agio, M. *Phys. Rev. E* **2006**, *74*, 036603.
- (20) Dorado, L. A.; Depine, R. A.; Míguez, H. *Phys. Rev. B* **2007**, *75*, 241101(R).
- (21) Nair, R. V.; Vijaya, R. *Phys. Rev. A* **2007**, *76*, 053805.
- (22) Schutzmann, S.; Venditti, I.; Proposito, P.; Casalboni, M.; Russo, M. V. *Opt. Express* **2008**, *16*, 897.
- (23) Dorado, L. A.; Depine, R. A.; Lozano, G.; Míguez, H. *Opt. Express* **2007**, *15*, 17754.
- (24) Dorado, L. A.; Depine, R. A.; Schinca, D.; Lozano, G.; Míguez, H. *Phys. Rev. B* **2008**, *78*, 075102.
- (25) Checoury, X.; Enoch, S.; López, C.; Blanco, A. *Appl. Phys. Lett.* **2007**, *90*, 161131.

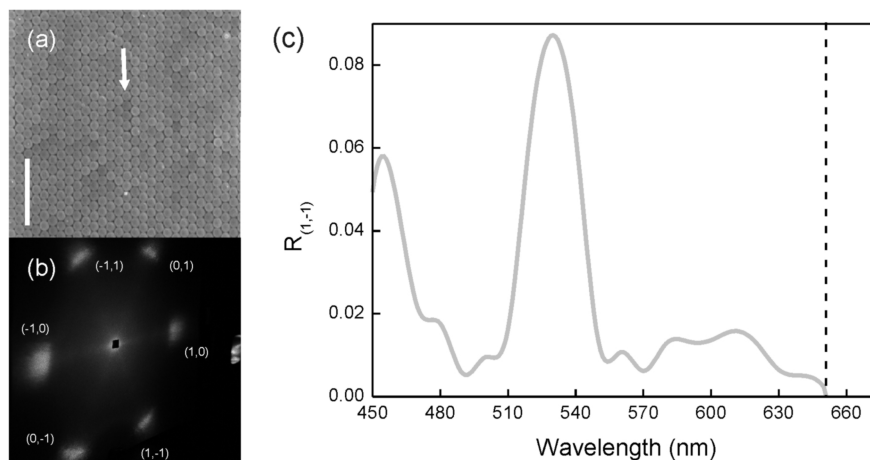


Figure 1. (a) SEM micrograph of the surface of an artificial opal film made of $0.75 \mu\text{m}$ polystyrene spheres. Scale bar is $5 \mu\text{m}$. Vertical arrow indicates the growth direction. (b) Diffraction pattern of reflected beams projected on a screen parallel to the surface of the artificial opal film for $\lambda = 532 \text{ nm}$. (c) Measured reflection efficiency of the diffracted channel $(1, -1)$. Vertical dashed line indicates the onset of diffraction for reflected modes; see ref 24 for details.

Herein, we present a detailed description of the structure of artificial opals grown by EISA on nonhorizontal substrates. From the analysis of the optical response in a wide spectral range ($0.4 \leq a/\lambda \leq 2$) of both the normal and off-normal diffracted beams, we attain detailed information on the geometry of the lattice, which serves us to draw a more realistic description of colloidal crystals in which the originally spherical scattering centers are now distorted and placed in a rhombohedral three-dimensional assembly. We also analyze the effect on the photonic band structure of this distortion, which turns out to be significant.

Methods

Sample Preparation. Artificial opal films analyzed in this work were grown using a variation of the vertical deposition method developed by Colvin and co-workers.⁶ They are formed as a result of the evaporation of the liquid phase of a colloidal dispersion at the contact line with the suspension meniscus. As a result, a solid film is deposited onto a substrate placed in a nonhorizontal position within a beaker containing a dispersion of commercial polystyrene particles (IKERLAT; average diameter of 750 nm , after transmission electron microscopy measurements; polydispersity of about 3%). The substrates employed were glass microscope slides ($12 \text{ mm} \times 76 \text{ mm}$), which were cleaned with doubly distilled water, acetone, carbon tetrachloride, and a 4:1 (v/v) $\text{H}_2\text{SO}_4/\text{H}_2\text{O}_2$ solution before being dried under a N_2 flow. These substrates were then dipped into a cylindrical glass beaker (inner diameter, 25 mm ; volume, 25 mL) containing the polystyrene colloidal suspensions (15 mL) with a concentration of $0.05 \text{ vol } \%$. Subsequently, the beakers were placed in an oven at $50 \text{ }^\circ\text{C}$, and water was evaporated for 4 days. Under these specific conditions, the spheres in the film tend to self-organize and form a high-quality colloidal crystal on a $12 \text{ mm} \times 16 \text{ mm}$ area of the substrate. Figure 1a shows a scanning electron microscopy (SEM) image of the outer (111) plane of a colloidal crystal film, where it can be observed the spheres ordered in a triangular lattice. In this paper, round brackets indicate a specific crystalline plane, square brackets a particular direction, and the notation $\{hki\}$ a set of planes equivalent to (hki) by the symmetry of the lattice.

Results and Discussion

Analysis of Off-Normal Diffraction. The onset of a diffracted mode exiting from the surface of the opal film only depends on the geometry of the two-dimensional arrangement shown in Figure 1a and the refractive index of the diffraction

medium, n . Each diffracted mode is labeled by the couple of integer indexes (p, q) which serves to identify a particular diffracted mode in the vector basis used, which is defined in ref 24. For a triangular lattice and normal incidence, this onset is given by the expression:

$$\frac{a}{\lambda} \geq \frac{\sqrt{2}}{n} \sqrt{p^2 + \frac{(2q + p)^2}{3}} \quad (1)$$

According to this equation, diffraction in air starts at $a/\lambda \sim 1.63$ for the six modes labeled as $(1, 0)$, $(0, 1)$, $(1, -1)$, $(-1, 1)$, $(-1, 0)$, and $(0, -1)$. The diffraction cutoff wavelength (λ_c) is indicated as a vertical dashed line in Figure 1c, in which we show actual measurements of the diffracted beam intensity for a specific diffracted channel, namely, $(1, -1)$. In Figure 1b, a photograph of the diffraction spots rising from the opal film can be observed on a screen parallel to the surface of the lattice. From the experimental value of the diffraction cutoff wavelength λ_c and using eq 1, we can extract information on the periodicity along the (111) plane. The average center to center distance between neighboring spheres in the triangular arrangement turns out to be $0.75 \mu\text{m}$, which agrees with the particle diameter measured from transmission electron microscopy images of nonpacked spheres.

Analysis of Specular Reflectance at Normal Incidence. On the other side, specular reflectance measurements were performed for a wide range of wavelengths. In order to do so, we used a Fourier transform infrared spectrophotometer (Bruker IFS-66) attached to a microscope. A $4\times$ objective with a numerical aperture of 0.1 (light cone angle of 5.7°) was used to irradiate the lattices and collect the reflected light at quasinormal incidence with respect to its surface. In this case, simulated reflectance spectra were calculated using the vector Koringa–Kohn–Rostoker (KKR) wave calculation method in its layer version.²⁶ In principle, the model structure considered was a close-packed FCC lattice of spheres of dielectric constant $\epsilon_s = \epsilon_r + i\epsilon_i$ embedded in air; the ϵ_i value is related to the amount of disorder.²⁷ In all the calculations, numerical convergence was obtained using a

(26) Stefanou, N.; Yannopoulos, V.; Modinos, A. *Comput. Phys. Commun.* **1998**, *113*, 49. Stefanou, N.; Yannopoulos, V.; Modinos, A. *Comput. Phys. Commun.* **2000**, *132*, 189.

(27) Dorado, L. A.; Depine, R. A. *Phys. Rev. B* **2009**, *79*, 045124.

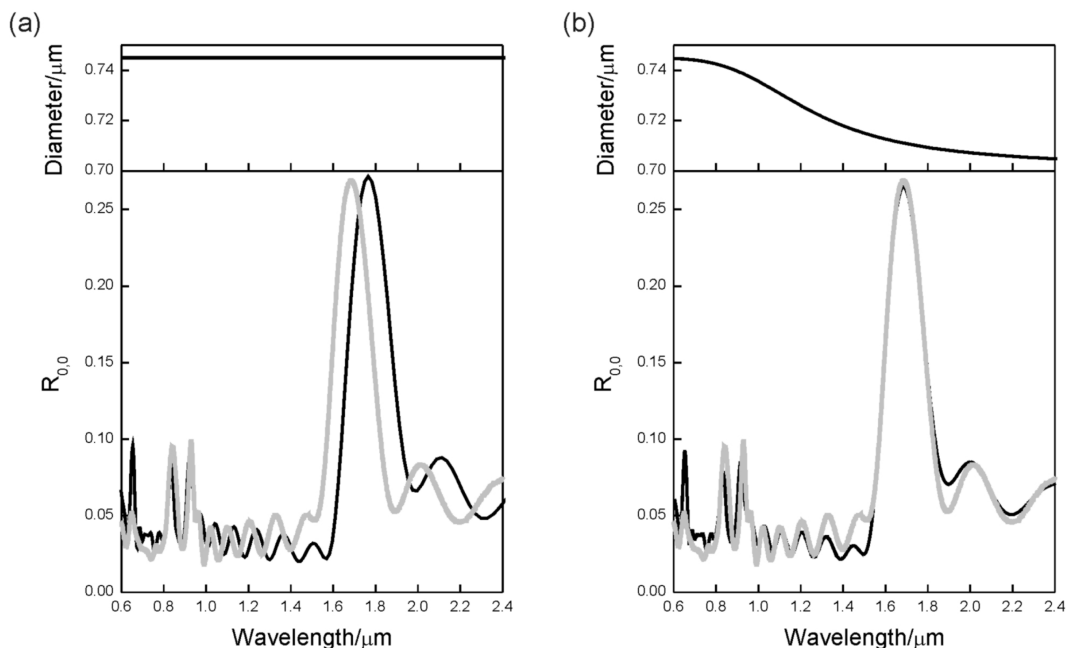


Figure 2. Measured (gray line) and calculated (black line) specular reflectance spectra when a constant (a) and a function diameter (b) are considered. Calculations were done considering crystal thickness as seven layers and the dielectric constant of spheres $\epsilon_s = 2.5 + i0.13$. We have used a smaller value of the ϵ_i parameter (0.08) in the higher energy spectral range, which represents the different effects imperfections have on the different wavelength ranges.

maximum value of the angular momentum $L_{\text{MAX}} = 9$ in the spherical wave expansion and 41 plane waves. Measurements and calculations are presented in Figure 2a. These calculations are done in reduced frequency units $2\pi d/\lambda$, with d being the diameter of the packed spheres. The gray line in Figure 2a is the reflectance measured from a seven layer colloidal crystal, whereas the black one is the theoretical spectrum attained when the interparticle distance between spheres is taken to be $0.75 \mu\text{m}$, as extracted from the off-normal diffraction measurements. It is clearly seen that, although a good agreement with experiment is found for both the number of peaks and their position in the high energy range (i.e., $\lambda \leq 1.05 \mu\text{m}$), the position of the lower energy reflection peak is mismatched. This maximum is also known as the Bragg peak, and it is the result of the opening of a stop band between the lowest energy photonic bands along the Γ -L direction in reciprocal space, which corresponds to the [111] direction in the real space of an FCC structure. In fact, an expression that combines Bragg and Snell laws can be used to estimate the effective refractive index of the colloidal crystal and the interplanar spacing between piled (111) planes based on the fitting of the angular shift of this peak.²⁸ This is the approach employed by Ishii et al. in ref 15. In our case, optimized fitting of specular reflectance in the complete spectral range is attained by reducing the interparticle distance as we move toward the lower energy range, as shown in Figure 2b, in which we also plot the function used to represent the variation of the sphere center to center distance used in the calculation versus wavelength. This function can be used to represent the distortion of the spheres only because the directions along which the spheres are compressed affect the optical properties in well-defined energy ranges. This justifies the use of a diameter function so that we force the interparticle distance to diminish as we move toward the lower energy range. Besides, it has been reported that imperfections have different effects on different wavelength ranges. Disorder in artificial opal films dramatically affects the optical

response in the high energy range.^{20,23} For this reason, the imaginary part of the dielectric constant, which is related to the amount of disorder, is not considered as a constant value during calculations. Specifically, we employed a smaller value of the ϵ_i parameter in the high energy spectral range (i.e., $\lambda \leq 1.05 \mu\text{m}$). Changes of ϵ_i as a function of λ permit adjustment of the intensity of the peaks but leave their spectral position unaltered. Similar optimized fittings were found for numerous artificial opals built of spheres with a wide range of sizes and made of both polystyrene and silica. In all cases, optical properties observed in the lower energy range cannot be fitted unless a contraction of approximately 5% of the distance between first neighbors is considered with respect to the value used to simulate the response at higher energy. Our results thus confirm that the commonly assumed close-packed FCC structure is actually compressed along directions that form an angle different from 90° with the [111] one, and that particles can still be considered to have contact points with their first neighbors contained in the (111) plane. The lattice distortion described is not easy to appreciate by SEM because the compression of the spheres is small and close to the error of the apparatus. This is probably the reason why it has never been reported.

A New Proposed Structure for Artificial Opal Films. The results of our optical analysis are in good agreement with the conclusions recently reported by Marlow and Popa, who have described the drying of an opal film as a multiple stage process¹⁶ during which the Bragg peak position blue-shifts as a consequence of the physical compression of the spheres. Such a compression would transform the ideal hard-sphere opal with pointlike sphere contacts into an opaline arrangement with circlelike contact surfaces. Based on our interparticle distance estimations, we propose a structure for actual opal lattices in which the colloids are assumed to preserve its spherical shape except in those directions along which they touch a first neighbor not contained in the same [111] plane. Such structure is a rhombohedral lattice that must be described using a set of primitive lattice vectors

(28) López, C.; Blanco, A.; Míguez, H.; Meseguer, F. *Opt. Mater.* **1999**, *13*, 187.

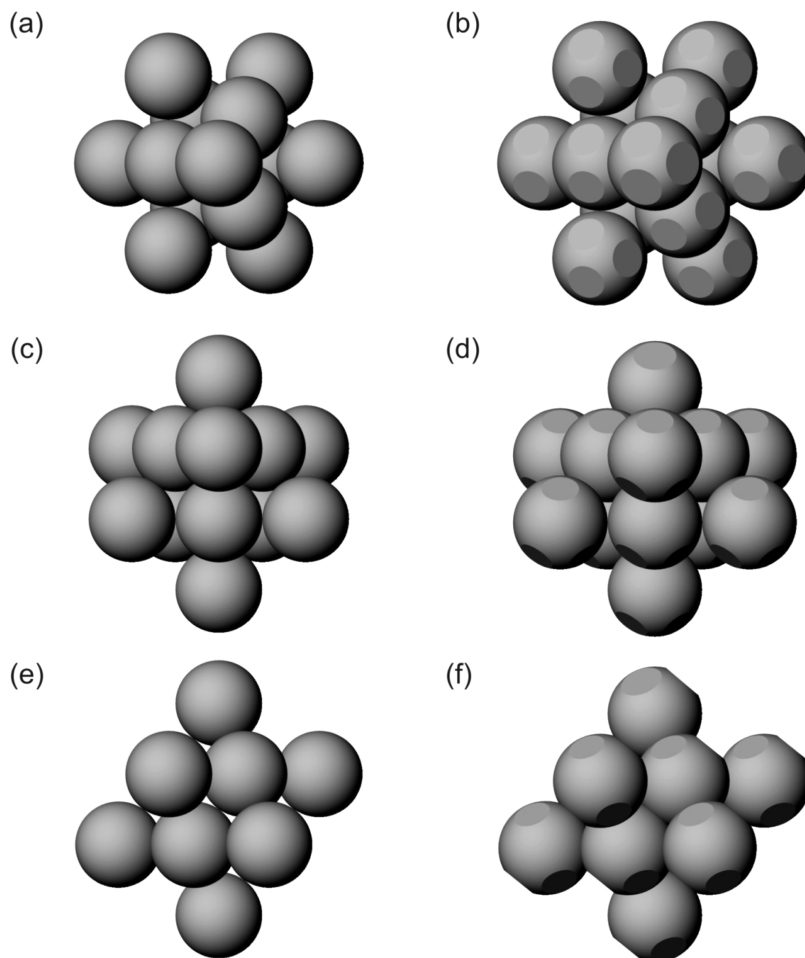


Figure 3. Views of the conventional cell for an FCC (left) and a rhombohedral (right) structure along the [111] (a,b), [11-2] (c,d), and [1-10] (e,f) directions.

(α, β, β) , (β, β, α) , and (β, β, α) . Introducing the center to center distance between the colloidal particles, A , and the angle between the primitive lattice vectors, θ , the components α and β are given by

$$\alpha = \frac{A}{3} \left(\sqrt{1 + 2\cos \theta} - 2\sqrt{1 - \cos \theta} \right)$$

$$\beta = \frac{A}{3} \left(\sqrt{1 + 2\cos \theta} + \sqrt{1 - \cos \theta} \right) \quad (2)$$

The distance A is equal to the length of the primitive lattice vector, and the angle θ indicates the degree of compression or distortion. In the case of $\theta = 60^\circ$, the lattice forms an FCC structure, and, in the case of $\theta = 90^\circ$, a simple cubic structure. According to the results presented in Figure 2, real opaline structures are rhombohedral lattices characterized by an angle $\theta = 63^\circ$. This value is found by imposing to a rhombohedral lattice the distance between first neighbors along different directions extracted from the analysis of the optical response in the complete spectral range. A tentative scheme of the actual structure is shown in Figure 3, which shows the conventional cell for an FCC lattice (left) and for the proposed opal lattice (right). The ideal FCC structure shows pointlike sphere contacts, whereas the rhombohedral presents circlelike contact regions along certain directions. The interparticle distance in the FCC lattice is isotropic and equal to the diameter of the colloids, whereas for the distorted lattice it is anisotropic. In both cases, each sphere is tangent to the six that surround it in the (111) plane, as it is clearly shown in Figure 3a,b.

It can also be observed in Figure 3e,f that the rectangular arrangement that exists in the FCC plane family $\{110\}$ turns to be an inclined parallelogram in the distorted lattice. It must be remarked that a small compression can also exist within the (111) plane in real samples, as suggested by previous fine experiments of liquid crystal infiltration within opal films.¹³ This compression would be around 10 times smaller than the compression existing in oblique directions and could be detected by performing very precise determinations of the diffraction cutoff wavelength for the different diffracted beams. This would also give rise to circular contact regions of very small diameter between spheres in such a plane. For the purpose of analyzing the main implications resulting from a distortion of the sort and magnitude detected, we will assume contact points between spheres contained in the plane as drawn in Figure 3b, d, and f. The distortion found gives rise to relevant modifications of the reciprocal lattice. This is fully illustrated in the Supporting Information. In the insets of Figure 4, we show the first Brillouin zone (FBZ) of the cubic close packed structure (left) and the actual distorted lattice (right). The FBZ for an ideal FCC arrangement is a truncated octahedron, with eight hexagonal and six square regular faces. For a structure with the geometry of a real opal lattice, the FBZ is a distorted truncated octahedron. It also has eight hexagonal and four quadrilateral faces, but none of them are regular. Two sets of identical hexagonal facets can be distinguished, with one containing two and another containing four of them. There is therefore a high symmetry point that does not exist in the FCC packing, labeled as

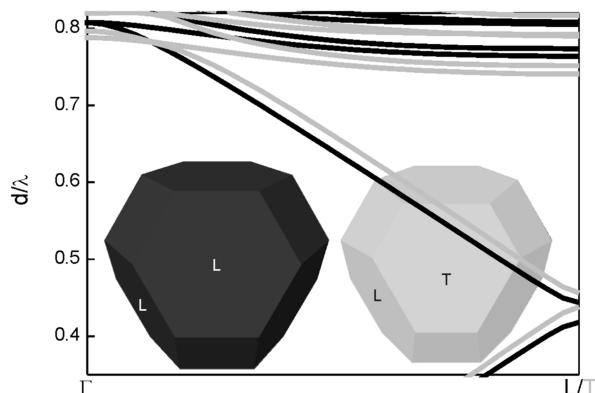


Figure 4. Calculated photonic band structure for an FCC and a rhombohedral ($\theta = 63^\circ$) structure consisting of dielectric polystyrene spheres ($\epsilon_s = 2.5$) in an air background along Γ -L (back line) and Γ -T (gray line) directions. Γ is the center of the FBZ.

T, at the center of two of the hexagonal facets. On the other side, there is just one set of similar quadrilateral facets. What is relevant in terms of the optical analysis of the structures is that the experimentally accessible direction in the distorted lattice is actually Γ -T rather than the commonly assumed Γ -L.

Effect of Fine Structural Features on the Photonic Band Structure. The effect of the distortion on the photonic band structure was also studied. In order to do so, calculations were accomplished using the MIT Photonic-Bands (MPB) free software.²⁹ The photonic band structure gives us information about the propagation properties of electromagnetic radiation within an infinite photonic crystal. It is a representation in which the available energy states are plotted as a function of propagation direction. The distorted lattice was simulated by considering a lattice of spherical scattering centers that overlap only in directions parallel or oblique to the [111] one, but that have only one contact point with first neighbors contained in the [111] plane. Although the full photonic band structure for up to 35 bands is presented as Supporting Information for both the FCC and the proposed rhombohedral lattices,³⁰ herein we focus on the modes attained for the lowest energy bands for two specific directions, Γ -L in the FCC lattice and Γ -T in the rhombohedral. Calculations were made considering spheres of $\epsilon_s = 2.5$ in air, and the results are plotted in reduced units of d/λ , with d being the nominal sphere diameter of the spheres, that is, the distance between spheres contained in the same (111) plane along which no contraction occurs. Please notice that the value of this parameter is the same for both the FCC and the rhombohedral structures, which allows the comparison between them. It can be clearly seen that for the energy range between $d/\lambda = 0.418$ and $d/\lambda = 0.443$ no modes are found for the FCC lattice along Γ -L. For the case of the rhombohedral lattice, the pseudogap opens up at higher

energies, that is, between $d/\lambda = 0.438$ and $d/\lambda = 0.456$, as a result of the contraction of the (111) planes. Also, the expected gap to midgap ratio for the actual structure is expected to be 4.0% rather than the commonly assumed 5.8%, thus around 30% narrower. It is precisely this stop band that is the one associated to the primary reflectance maximum in the experimental reflectance spectrum (see Figure 2). The reason why such an effect has not been reported experimentally lies, in our opinion, in the fact that artificial opal films are finite and imperfect lattices. For a given crystal size, intensities of around one-half of the values expected for the ideal structures are measured. Both the finite size and the imperfections broaden the spectral width and reduce the intensity of the reflectance peak. For this reason, any strict comparison to the gap to midgap ratio values extracted from band structure calculations has not been possible. Also, it is interesting to notice that the compression of the colloids in the arrangement causes the narrowing of the spectral separation between the region of low dispersion bands, observed at around $d/\lambda = 0.764$ for the FCC and $d/\lambda = 0.741$ for the rhombohedral structure, and the position of the lower energy pseudogap. This separation is in much better agreement with the spectral positions of the peaks associated to each group of bands observed experimentally.

Conclusions

In conclusion, we have shown experimental optical evidence of the existence of lattice distortion in artificial opal films. We have thoroughly analyzed the effect of fine structural features on the optical response to conclude that, rather than the generally assumed FCC lattice of spheres, opal films are better approximated by a rhombohedral assembly of distorted colloids. Interparticle distance of actual colloidal crystals coincides with the expected diameter for spheres belonging to the same close-packed (111) plane but differs significantly in directions oblique to the [111] one. We have also presented a full description of the real and reciprocal space representations of the proposed distorted lattice, as well as of its photonic band structure.

Acknowledgment. This research has been funded by the Spanish Ministry of Science and Innovation under Grant MAT2007-02166 and Consolider HOPE CSD2007-00007, Junta de Andalucía under Grant FQM3579, the Consejo Nacional de Investigaciones Científicas y Técnicas (CONICET, Argentina), and the Agencia Nacional de Promoción Científica y Tecnológica (PICT-11-1785). G.L. thanks CSIC for funding through an I3P scholarship.

Supporting Information Available: Calculated optical reflectance with and without taking into account the material dispersion; views of the first Brillouin zone of the FCC and rhombohedral lattice; calculated photonic band structure for an FCC and a rhombohedral lattice along several directions. This material is available free of charge via the Internet at <http://pubs.acs.org>.

(29) Johnson, S. G.; Joannopoulos, J. D. *Opt. Express* **2001**, *8*, 173.

(30) More details about the photonic band structures of compressed artificial opals can be found in Harada, M.; Ishii, M.; Nakamura, H. *Jpn. J. Appl. Phys.* **2009**, *45*, 676.